AIAA 81-4200

Transonic Swept Wings Studied by the Lifting-Line Theory

H. K. Cheng* and S. Y. Meng†
University of Southern California, Los Angeles, Calif.
and
R. Chow‡
Grumman Aerospace Corporation, Bethpage, N.Y.
and
R. C. Smith§
NASA Ames Research Center, Moffett Field, Calif.

Transonic swept wings are analyzed as a lifting-line problem under a small-disturbance approximation. Basic concepts and principal results of the asymptotic theory are discussed. The study focuses on straight oblique wings and V-shaped swept wings, of which the local centerline curvature can be equated to zero. The three-dimensional (3-D) perturbation of the nonlinear component flow admits a similarity flow structure but requires that all wing sections are generated from a single airfoil profile; the reduced 2-D problems in this case are solved only once for all span stations. Examples of solutions involving high subcritical and slightly supercritical component flows are demonstrated and compared with surface pressure data from 3-D computer codes based on the full-potential equation (FLO 22). Except in the neighborhood of leading edges, where the small-disturbance assumption breaks down, and in the vicinities of wing tips and the symmetry plane, where neither the theory nor the 3-D codes may claim full validity, reasonable agreement is consistently found. The explicit results from the upwash analysis, along with the similarity flow structure, provides a rational approach to the control of 3-D effects in transonic aerodynamic design studies.

I. Introduction

OUR understanding in the aerodynamics of wing sweep and its use to control the compressibility effect have been limited in the past mostly to problems in the linear flow regimes.[1-5] Current interest in aircraft wing design has focused on adopting two-dimensional (2-D) supercritical airfoil data,[6-11] where the flow in this domain is nonlinear with a transonic flow component. The problems of sweep and the 3-D corrections to mixed component flows have recently been studied by Cheng, Cook, and others[12-20] as extensions of the classical lifting-line theory.[21,22] As a sequel to Cheng and Meng's work,[15,16] this paper will present a more complete discussion of its applications, considering examples not previously analyzed. An essential part of the study is comparisons with solutions generated from existing full-potential computer codes; certain apsects for future improvement of the latter will also be brought out.

In the domain of interest, the flowfield far from the wing section should pertain to a high subsonic, or linear sonic, outer flow, which is representable in the leading approximation by a solution to the Prandtl-Glauert equation corresponding to a swept lifting line. Thus, the theoretical treatments[12-20] mentioned have genesis in Prandtl's original lifting-line idea,[21,22] even though the corresponding inner problem is nonlinear and may involve an embedded supersonic region. Apart from gaining a better physical insight and a greater simplicity in the analysis, the approach reflects a desire for implementing the current computer-oriented 3-D methods[23-29] which, though being very powerful, share the well-known problem of trading accuracy with computer cost and storage requirements. One obvious contribution to which the approach may lead is providing an asymptotic basis upon which numerical results from current 3-D codes can be correlated and their adequacy tested.

The asymptotic theory underlying the present study has been given quite thoroughly in Cheng and Meng's work.[15,16] A similar formulation has been developed by Cook for straight oblique wings.[20] Most high aspect ratio wing analyses in classical literature are concerned with unyawed, straight wings, and were tied closely to Prandtl's lifting-line theory; documented works in this category are numerous (see review by Jones and Cohen[3]). Some of the earlier works[30-33] possess features which are quite relevant to the present study, and have been reviewed along with transonic lifting-line works[17-20] in Ref. 34.

Section II will discuss the basic concepts of the theory and their physical implications. The distinction from classical lifting-line analyses will be apparent. In order to allow a fuller discussion of the solution examples and their comparison with full-potential solutions (see Sec. IV), mathematical details described in Sec. III will be kept to a minimum, of which readers are referred to the published works.[14-16]

A limitation of the present approach is the assumption of a smooth centerline, which obviously breaks down in the vicinity of the apex of a conventional (symmetric) swept wing. The example analyzed will show, however, that this region of nonuniformity is limited in extent; agreement with the full-potential solution remains reasonable at span stations well within one root chord from the symmetry plane. An important property uncovered from the study of Refs. 14-16 is the similarity flow structure which permits the reduced problem to be solved only once for all span stations. Interestingly, this property remains even after the small-disturbance assumption is removed, as demonstrated by a formulation based on full-potential equations in Ref. 36.

The following analysis will deal mainly with centerlines composed of one or two straight segments such as a straight oblique wing or a V-shaped swept wing, respectively. All examples studied in this paper are shock-free.

Received Aug. 20, 1980; revision received March 18, 1981.

*Professor, Dept. of Aerospace Engineering. Member AIAA.
†Research Assistant; presently at Hydrodynamics Division, Rockwell International Corporation.
‡Staff Scientist, Research Department. Member AIAA.
§Senior Research Scientist, Aeronautics Division. Member AIAA.

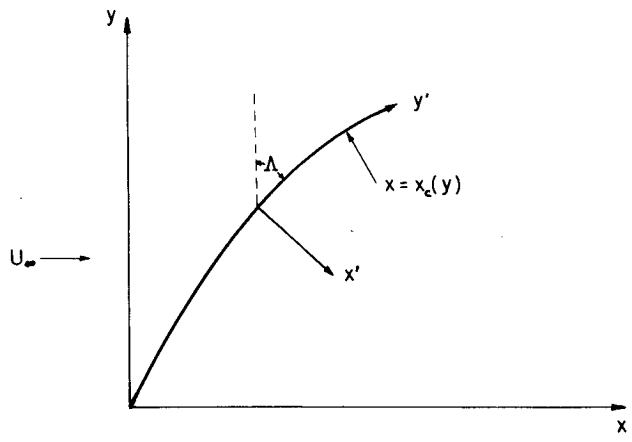

Fig. 1 Cartesian and orthogonal curvilinear coordinates in the wing plane $z=z'=0$.

II. Essential Elements of the Theory

Following Prandtl's lifting-line theory for high aspect ratio wings,[21] two (asymptotically) distinct flow regions are considered: 1) a nearly planar (2-D) region next to the wing section with a streamwise length scale comparable to the typical wing chord c_0; 2) a fully 3-D domain with its lateral size comparable to the wing half-span b. These are the inner and outer regions of the singular perturbation theory.[22] Since the aspect ratio $\mathcal{R}_l \equiv 2b/c_0$ is high, the wing, along with its near wake, is perceived in the outer flow region as a lifting line—a line of singularities, to be more precise.

Students of classical aerodynamics are familiar with the idea that the velocity induced by the trailing vortex sheet causes a change in the local flow angle, proportional to $\mathcal{R}_l^{-1}$. Implicit are the assumptions that the flow around the wing section is strictly planar, and that the induced velocities defined in the classical sense remain bounded. These stipulations do not hold for a swept wing with a nonvanishing sweep angle. The distinct features brought out in the analysis for swept wings are described below.

Centerline Curvature and Spanwise Density Variation

The partial-differential equation governing the component flow around the wing section must be corrected for compressibility effects and for the 3-D effect due to a nonvanishing local curvature of the centerline of the planform, $d\Lambda/dy'$ (see Fig. 1 for coordinates and definition of Λ). The former includes a correction resulting from the spanwise density variation (see Sec. III).

Spanwise Component of Wake Vorticity

Owing to the sweep, the wake vorticity just behind the trailing edge has a nonvanishing component along the centerline. Thus, the tangential velocity component normal to the centerline has a nonvanishing jump across the trailing vortex (TV) sheet.[12,13] Therefore, the solution to the reduced inner problem is no longer planar, but must be corrected in both the partial-differential equation and in the boundary condition on the wing trace, i.e., the TV sheet.

Logarithmic Upwash

The induced upwash effect on the wing section characteristics is determined from the behavior of the outer (lifting-line) solution in the vicinity of the lifting line. In approaching the latter, the outer solution is dominated by that of a line vortex representing the effect of bound vortices on the wing. Unlike the classical theory for unyawed straight wings,[21,22] the induced upwash (obtained after subtracting out the vortex singularity) approaches infinity like the logarithm of the distance from the lifting line. This singular behavior is needed for matching with the corresponding (far-field) behavior of the inner solution [see Eq. (14b)]. The strength of this singularity is proportional to $\tan\Lambda(d\Gamma/dy')$, where Γ is the circulation, hence, to the sweep angle and the shedded vorticity at the span station in question. Upon matching with the inner solution, the logarithm yields an additional term to the upwash proportional to $\ell n(2b/c_0) = \ell n\, \mathcal{R}_l$, which dominates over the remaining finite part of the upwash, W_l. In view of its linear dependence on $d\Gamma/dy'$, it may rightfully be regarded as a contribution of the near wake.

The origin of the logarithmic singularity can be understood from a decomposition of the locally shedded trailing vorticity into two components, parallel and normal to the centerline ($x'=0$).[34] The component parallel to $x'=0$ gives a logarithmically infinite upwash as $x' \to 0^+$.

Logarithmically large upwash corrections occur also in unsteady problems and in problems involving curved centerlines. Analyses of the outer flow behavior near the centerline has been described for a straight oblique wing in Ref. 12 for incompressible flow, and for a wing with straight as well as curved centerline in the transonic regime in Refs. 15 and 16. (Results obtained from the curved lifting-line theory for incompressible flows in the steady and unsteady cases have not yet been published.)

Transonic Swept-Wing Problems

For problems involving a transonic flow component ($M_n = M_\infty \cos\Lambda \sim 1$), the nonlinearity familiar in the transonic flow study must be adequately treated in the equation governing the inner flow. If the freestream is also transonic, i.e., $M_\infty \sim 1$, the conditions $M_n \sim M_\infty \sim 1$ implies that the swept angle must remain sufficiently small in the nonlinear regime. Denote the absolute angle of attack or the thickness ratio of the wing section, whichever is larger, by α. The range of sweep must be such that $(1-M_n^2)/\alpha^{2/3} = 0(1)$, in order to keep the component flow nonlinear. This requires $\Lambda = 0(\alpha^{1/3})$. Interestingly, the smallness in Λ renders the effect of the spanwise component of the trailing vorticity negligible in the off-wing boundary condition, but the logarithmic upwash associated with this spanwise trailing vorticity remains a dominating feature in the transonic problem.

III. Reduced Transonic Problems and Key Equations

Basic Parameters and Governing Equations

We consider high subsonic flight near the speed of sound. The component flow in this case is necessarily nonlinear and may become supercritical. If the wing sections are assumed to be thin, this component flow at each span station will be controlled by the transonic similarity parameter based on the component Mach number $M_n \equiv M_\infty \cos\Lambda$

$$K_n \equiv (1-M_n^2)/\alpha^{2/3} M_n \tag{1}$$

familiar from the transonic small-disturbance theory.[37-39] The sweep range of interest is that which will keep K_n at order unity, while M_∞ does not exceed 1. This requires

$$\Theta \equiv \frac{\Lambda}{\alpha^{1/3}} = 0(1) \tag{2}$$

The parameter Θ may be referred to as a reduced sweep angle. Essential to the development is a reduced aspect ratio, the reciprocal of which is

$$\epsilon \equiv \frac{1}{\alpha^{1/3} \mathcal{R}_l} \tag{3}$$

The asymptotic analyses of Refs. 14-16 pertain to the limit $\epsilon \to 0$, holding K_n and Θ (as well as $\alpha^{1/3}\epsilon^{-1}$) fixed. With the additional requirement, $M_\infty < 1$, the foregoing requirements on K_n and Θ can be replaced by

$$\Theta^2 < K_n = O(1) \tag{4}$$

We shall summarize the key equations for the reduced inner problem using a system of curvilinear orthogonal coordinates (x',y',z') shown in Fig. 1. Introduce the inner reduced variables

$$\begin{aligned} \hat{x} &\equiv 2x'/c_0 & \hat{z} &\equiv 2M_n\alpha_1^{1/3}z'/c_0 \\ \hat{y} &\equiv y'/b & \hat{\phi} &\equiv 2\phi/\alpha_1^{2/3}U_n c_0 \end{aligned} \tag{5}$$

as suggested by the similitude of the transonic small-disturbance theory, with $c_0/2$ taken to be the reference length scale and $U_n \equiv U_\infty \cos\Lambda$ as the reference velocity.[37,38] In the above equation, ϕ is the perturbation velocity potential and α_1 is simply α/M_n.

For swept wings with straight centerlines, the full-potential equation can be reduced for small ϵ under Eq. (4) to[14-16]

$$\frac{\partial}{\partial\hat{x}}\left[K_n\hat{\phi}_{\hat{x}} - \frac{\gamma+1}{2}\hat{\phi}_{\hat{x}}^2\right] + \hat{\phi}_{\hat{z}\hat{z}} = 2\Theta\epsilon\hat{\phi}_{\hat{x}\hat{y}} \tag{6}$$

with a remainder of order ϵ^2. The left-hand members are the familiar terms in the 2-D von Kármán equation,[37] and the term of order ϵ on the right-hand side is the 3-D compressibility correction for the spanwise density variation. The pressure coefficient can be computed from $\hat{\phi}$ as

$$C_p \equiv \frac{p-p_\infty}{\frac{1}{2}\rho_\infty U_\infty^2} = -2\cos^2\Lambda\alpha_1^{2/3}\hat{\phi}_{\hat{x}} \tag{7}$$

with a remainder comparable to ϵ^4. Note that as long as $\Theta = 0(1)$, C_p is unaffected directly by the spanwise velocity $\hat{\phi}_{\hat{y}}$. The inclusion of M_n in the definition of K_n leads to an improvement in predicting the critical speed, hence, the wave pattern near the sonic boundary, as ascertained analytically by Cheng and Meng.[16] We point out that most $\cos\Lambda$ factors appearing in Eqs. (1-7), except that in $(1-M_n^2) = 1 - M_\infty^2\cos^2\Lambda$ of K_n, could be replaced by unity, consistent with the asymptotic theory. However, their retention will allow a greater range of sweep without sacrificing accuracy[15,16] (see also Refs. 23 and 38-40).

Inner Boundary Conditions

A nearly planar wing will be considered, of which the ordinate is expressible as

$$z' = \frac{c_0}{2}\left[\alpha\hat{Z}^{\pm}(\hat{x},\hat{y}) + \alpha^{1/3}\hat{Z}_B(\hat{y}) + \alpha\epsilon(\hat{x}-\hat{x}_0)\hat{I}(\hat{y})\right] \tag{8}$$

where $\hat{Z}^{\pm}$, $\hat{Z}_B$, and $\hat{I}$ are assumed to be of unit order and the "$\pm$" signifies the top and bottom surfaces. The unit-order functions $\hat{Z}_B$ and $\hat{I}$ represent an upward wing bend and a wing twist sufficient for controlling the unwarranted 3-D effects, such as the asymmetrical upwash induced by the wake vorticity behind an oblique wing.[5] The impermeable wing boundary condition can be transferred to the wing plane $(z=0)$, subject to an error of the order ϵ^2, as

$$\left(\frac{\partial\hat{\phi}}{\partial\hat{z}}\right)_w = \frac{\partial}{\partial\hat{x}}\hat{Z}^{\pm} + \epsilon\left[\Theta\frac{\mathrm{d}}{\mathrm{d}\hat{y}}\hat{Z}_B + \hat{I}\right] \tag{9}$$

where the subscript w refers to the wing surface.

The requirement of continuity of the normal velocity component and the pressure across the trailing vortex sheet (of zero thickness), leads to the condition that $\hat{\phi}_{\hat{x}}$ and $\hat{\phi}_{\hat{z}}$, not $\hat{\phi}_{\hat{y}}$, must be continuous across the wing trace. Hence, unlike the swept-wing problem in other flight Mach number ranges,[12,13] the inner transonic component flow can be treated without the vortical wake, subject to errors of the order ϵ^2.

Perturbation Analysis

The 3-D corrections in question represent a small peturbation of a 2-D transonic component flow; formally, we write

$$\hat{\phi} = \hat{\phi}_0(\hat{x},\hat{z};\hat{y}) + \epsilon\hat{\phi}_1(\hat{x},\hat{z};\hat{y}) + \ldots \tag{10}$$

with $\hat{\phi}_0$ and $\hat{\phi}_1$ satisfying

$$\left\{[K_n - (\gamma+1)\hat{\phi}_{0\hat{x}}]\frac{\partial^2}{\partial\hat{x}^2} + \frac{\partial^2}{\partial\hat{z}^2}\right\}\hat{\phi}_0 = 0 \tag{11a}$$

$$\left\{[K_n - (\gamma+1)\hat{\phi}_{0\hat{x}}]\frac{\partial^2}{\partial\hat{x}^2} + \frac{\partial^2}{\partial\hat{z}^2} - (\gamma+1)\hat{\phi}_{0\hat{x}\hat{x}}\frac{\partial}{\partial\hat{x}}\right\}\hat{\phi}_1 = 2\Theta\hat{\phi}_{0\hat{x}\hat{y}} \tag{11b}$$

To be sure, $\hat{\phi}_0$ is governed by the 2-D von Kármán equation in $\hat{x}$ and $\hat{z}$, and $\hat{\phi}_1$ satisfies a linear nonhomogeneous partial-differential equation (PDE) in $\hat{x}$ and $\hat{z}$. Throughout Eqs. (11), the spanwise variable $\hat{y}$ enters merely as a parameter. The wing boundary conditions are

$$\left(\frac{\partial\hat{\phi}_0}{\partial\hat{z}}\right)_w = \frac{\partial}{\partial\hat{x}}\hat{Z}^{\pm} \tag{12a}$$

$$\left(\frac{\partial\hat{\phi}_1}{\partial\hat{z}}\right)_w = \Theta\frac{\mathrm{d}}{\mathrm{d}\hat{y}}\hat{Z}_B + \hat{I} \tag{12b}$$

The 2-D system is elliptic or hyperbolic, depending on whether $K_n - (\gamma+1)\hat{\phi}_{0\hat{x}}$ is positive or negative. The coefficients $\hat{\phi}_1$ and $\hat{x}_1^D$ must allow a weak dependence on ϵ to accommodate the logarithmic upwash. Where a shock occurs, the shock boundary is described as

$$\hat{x} = \hat{x}_0^D(\hat{z};\hat{y}) + \epsilon\hat{x}_1^D(\hat{z};\hat{y}) + \ldots \tag{13}$$

The jump conditions transferred to the unperturbed shock boundary, $\hat{x} = \hat{x}_0^D$, are detailed in Refs. 14-16.

Solution Behavior Far from the Wing Section and Matching

Far from the wing section, the inner equations (11) admit the asymptotic behavior for large $\hat{\zeta} \equiv \hat{x} + i\sqrt{K_n}\hat{z}$

$$\hat{\phi}_0 \sim \frac{\hat{\Gamma}_0}{2\pi}\left[\tan^{-1}\left(\frac{\hat{x}}{\sqrt{K_n}\hat{z}}\right) + \frac{\pi}{2}\operatorname{sgn}\hat{z}\right] + \ldots \tag{14a}$$

$$\hat{\phi}_1 \sim \frac{\Theta}{2\pi\sqrt{K_n}}\hat{z}\frac{\mathrm{d}\hat{\Gamma}_0}{\mathrm{d}\hat{y}}\ln|\hat{\zeta}| - \hat{C}_1^i\hat{z} + \ldots \tag{14b}$$

The remainder in Eq. (14a) is dominated by terms comparable to a doublet, including $\hat{\Gamma}_0\hat{x}\ln|\hat{\zeta}|/|\hat{\zeta}|^2$ and $\hat{\Gamma}^2\hat{x}^3/|\hat{\zeta}|^4$ (see Ref. 16, Appendix 11). The remainder in Eq. (14b) is comparable to unity, including those of orders $(\ln|\hat{\zeta}|)^2$ and $(\ln|\hat{\zeta}|)$, one of which signifies a line source.[15,16]

The potential calculated from $\hat{\phi}_0 + \epsilon\hat{\phi}_1$ based on Eqs. (14), identified as the outer expansion of the inner solution, can be matched with the inner expansion of the outer solution calculated from $\hat{\phi}_0$ mentioned in Sec. II. The matching identifies the local circulation $\hat{\Gamma}_0(\hat{y})$ with that in the outer (lifting-line) solution, and determines the upwash correction $\hat{C}_1^i(\hat{y})$ from a finite part of the induced velocity at the lifting line $\bar{W}_1$ as[15,16]

$$\hat{C}_1^i(\hat{y}) = -\frac{1}{\sqrt{K_n}}\left[2\bar{W}_1 - \frac{\ln 2}{2\pi}\frac{\Theta}{\sqrt{K_n}}\frac{\mathrm{d}\bar{\Gamma}}{\mathrm{d}\hat{y}}\right] \tag{15}$$

The inner problem is thus reduced to solving Eqs. (11a) and (11b) with boundary conditions, Eq. (12), and the far-field behavior, Eqs. (14), using the results of matching, Eq. (15). The Kutta condition is essential and must be observed at the trailing edge for $\hat{\phi}_0$ as well as $\hat{\phi}_1$.

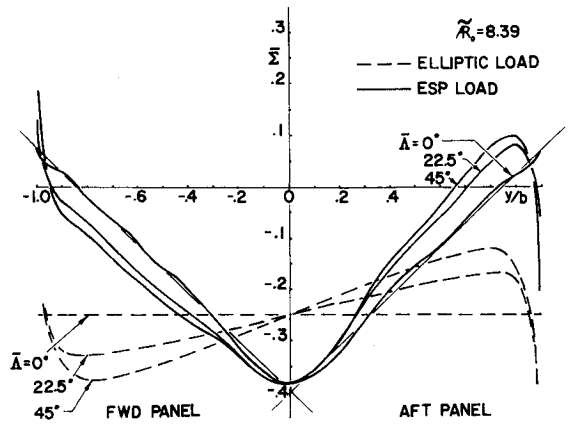

Fig. 2 Upwash function $\bar{\Sigma}$ illustrated for $\sqrt{1-M_n^2}\mathcal{R}_l = 8.39$ at three yaw angles for an elliptic and an extended span distribution in $\bar{\Gamma}_0$.

Induced Upwash on Swept Wings—Examples and Nonuniformity

To provide a more concrete idea on the induced upwash distribution and its difference from the classical result, we shall illustrate the function $\bar{W}_l$ [see Eq. (15)] for straight oblique wings with two types of loads, and for the V-shaped swept-forward and swept-back wings with elliptic loads. The function $\bar{W}_l(\bar{y})$ can generally be written in two parts[15,16,34]

$$\bar{W}_l = \tfrac{1}{2}(\bar{\Sigma} + \bar{\Sigma}_l^c) \tag{16}$$

where, with $\bar{m} \equiv \tan\bar{\Lambda} = \tan\Lambda/\sqrt{1-M_\infty^2}$,

$$4\pi\bar{\Sigma}(\bar{y}) = -\sin\bar{\Lambda}\bar{\Gamma}_0'(\bar{y})\,[2\ell n(\sqrt{K_n}/\epsilon) + 2$$

$$+ \ell n\,|(1-\bar{y}^2)\sec^2\bar{\Lambda}\,|] + \bar{\Gamma}_0'(\bar{y})\,\ell n\left|\frac{1-\bar{y}}{1+\bar{y}}\,\frac{1+\sin\bar{\Lambda}}{1-\sin\bar{\Lambda}}\right|$$

$$+ \int_{-1}^{1} \frac{\bar{\Gamma}_0'(\bar{y}_1) - \bar{\Gamma}_0'(\bar{y})}{\bar{y}_1 - \bar{y}}\,[1 - \sin\bar{\Lambda}(\bar{y})\,\mathrm{sgn}(\bar{y}_1 - \bar{y})]\,d\bar{y}_1 \tag{17a}$$

and $\bar{\Sigma}_l^c(\bar{y})$ is identically zero for a straight oblique wing, whereas for a V-shaped swept wing, it can be calculated from

$$4\pi\bar{\Sigma}_l^c(\bar{y}) = \int_{-1}^{1} \frac{\bar{\Gamma}_0(\bar{y}_1)}{(\bar{y}_1 - \bar{y})^2}\left[\frac{\bar{m}(\,|\bar{y}_1| - |\bar{y}|\,)}{\sqrt{\bar{m}^2(\,|\bar{y}_1| - |\bar{y}|\,)^2 + (\bar{y}_1 - \bar{y})^2}}\right.$$

$$\left. - \sin\bar{\Lambda}(\bar{y})\,\mathrm{sgn}(\bar{y}_1 - \bar{y})\right] d\bar{y}_1 \tag{17b}$$

where the subscript 0 refers to the leading (zeroth) approximation, and the prime signifies a derivative.

The asymmetrical upwash proportional to $\bar{\Gamma}_0'(\bar{y})$ in $\bar{\Sigma}$ is responsible for the unbalanced rolling moment of an oblique (pivoted) wing, unless twist, wing bend, or special pivot location is introduced in the design.[5,11-13] The extent to which this asymmetry depends on the pivoting angle $\bar{\Lambda}$ and on the span loading $\bar{\Gamma}_0(\bar{y})$ is illustrated in Fig. 2, where the upwash functions $\bar{\Sigma}(\bar{y})$ for oblique wings with an elliptic and an "extended-span distribution" are shown for $\bar{\Lambda} = 0$, 22.5, and 45 deg. (The extended span load considered has a root-bending moment equal to that of an elliptic load for the same lift but lesser drag[41]; the span, however, is 1.15 times that of the elliptic one.) These $\bar{\Sigma}$'s were computed from Eq. (17a) with $\bar{\Sigma}(\bar{y})$ normalized by the midspan value of $\bar{\Gamma}_0$, and the (reduced) aspect ratio taken to be such that $\sqrt{K_n}/\epsilon \approx \sqrt{1-M_n^2}\,\mathcal{R}_l \approx \sqrt{1-M_\infty^2}\,\mathcal{R}_l \sec\bar{\Lambda} \approx 8.4$.

The induced flow angle will also depend on the centerline geometry. Figure 3 shows the spanwise distribution of the normalized $\bar{\Sigma} + \bar{\Sigma}_l^c$ for symmetric swept-forward and swept-back wings at different degrees of sweep. It is assumed in the calculations that the span loading in the leading approximation, $\bar{\Gamma}_0(\bar{y})$, is elliptic, and that the product $\sqrt{1-M_\infty^2}$

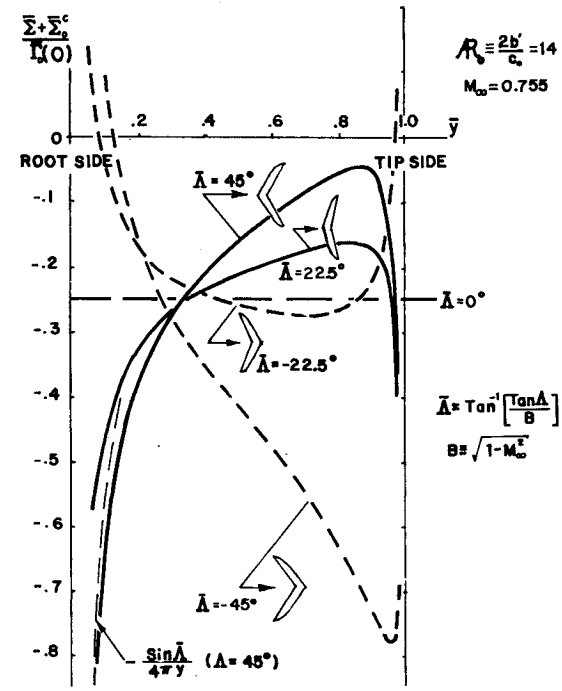

Fig. 3 Upwash function $\bar{\Sigma} + \bar{\Sigma}_l^c$ illustrated for elliptically loaded swept-forward and swept-back wings of $\mathcal{R}_l \approx 14$ at $M_\infty = 0.755$. Refer to text for conversion to other aspect ratio and Mach numbers.

$\mathcal{R}_l$ is 9.18, corresponding to $M_\infty = 0.755$ and $\mathcal{R}_l \approx 14$; results for five values of $\bar{\Lambda}$ (0, ±22.5, and ±45 deg) are shown. At $M_\infty = 0.775$, $\bar{\Lambda} = \pm 22.5$ and ±45 deg corresponds to $\Lambda = \pm 15.2$ and ±33.33 deg, respectively. The need for a washout on a swept-back wing is quite evident from the large reduction in $|\bar{\Sigma} + \bar{\Sigma}_l^c|$ near the tip shown. The usefulness of adopting a forward sweep ($\bar{\Lambda} < 0$) to revert the above effect (and to enhance maneuverability in roll) is also quite apparent from Fig. 3. In the outer portion of the swept-back wing, the upwash behavior is similar to that on the downstream panel of a straight oblique wing. Near the apex ($\bar{y} = 0$) of the swept-back wing, the induced upwash is negative, i.e., a downwash, and becomes unbound as $\bar{y} \to 0$ like

$$\bar{\Sigma}_l^c \sim -\bar{\Gamma}_0(0)\,(\sin\bar{\Lambda}/4\pi\bar{y}) \tag{18}$$

which corresponds to the velocity induced by the bound vortex on the opposite wing panel. (Compare the thin dash curve with the corresponding $\bar{\Sigma} + \bar{\Sigma}_l^c$ in Fig. 3.)

Similarity Flow Structure

Owing to the linearity, the 3-D correction $\epsilon\hat{\phi}_l$ can be decomposed into separate parts. There is an important class of wing surface geometry, for which each of these (properly scaled) separate parts have similarity solutions independent of $\hat{y}$, as does the basic solution $\hat{\phi}_0$. The reduced 2-D equation system in this case can be solved once for all span stations. This wing class requires that the wing section at each span station be generated from the same airfoil profile, keeping the same thickness ratio and incidence. That is, the function of $\hat{Z}^{\pm}(\hat{x},\hat{y})$ of Eq. (8) is required to conform to

$$\hat{Z}^{\pm} = \hat{c}(\hat{y})\,\tilde{Z}^{\pm}(\hat{x}/\hat{c}) \tag{19}$$

where $\hat{c}(\hat{y}) \equiv c(\hat{y})/c_0$. Implicit in Eq. (19) is that the centerline $\hat{x} = \hat{z} = 0$ is the common straight axis for the similar wing sections at different span stations. The location of this straight axis in percentage chord may, however, be arbitrarily set.

The similarity variables used are

$$\tilde{x} \equiv \hat{x}/\hat{c} \quad \tilde{z} \equiv \hat{z}/\hat{c} \quad \tilde{y} \equiv \cos\Lambda\hat{y} \approx \hat{y} \quad \tilde{\phi} \equiv \hat{\phi}/\hat{c} \tag{20}$$

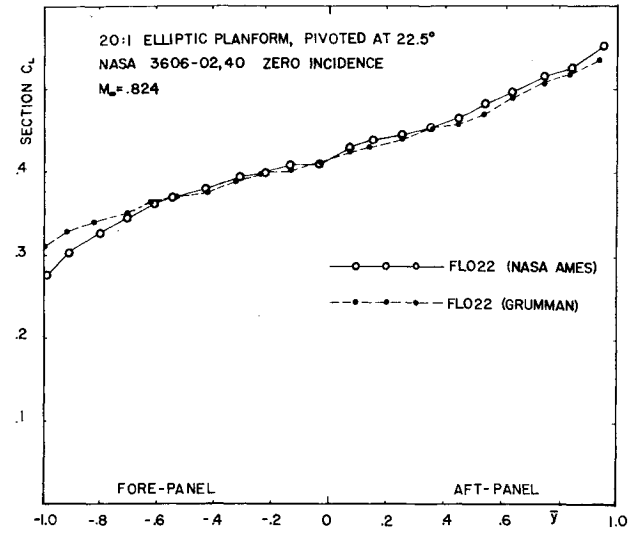

Fig. 4 Spanwise distribution of sectional lift coefficient computed for an oblique wing by solutions to the full-potential equation (FLO 22) from two sources.

The similarity flow structure admissible under Eq. (19), with due allowance for the upwash correction for an arbitrary loading, is given by

$$\tilde{\phi}=\tilde{\phi}_0(\bar{x},\bar{z})+\epsilon\Theta\hat{c}'\tilde{\phi}_1(\bar{x},\bar{z})-\epsilon\sqrt{K_n}\tilde{C}_l^i\bar{z}$$
$$+\epsilon[\sqrt{K_n}\tilde{C}_l^i(\bar{y})+\hat{I}(\bar{y})+\Theta\hat{Z}_B'(\bar{y})]\tilde{\phi}_2(\bar{x},\bar{z}) \qquad (21)$$

where $\hat{c}'\equiv d\hat{c}/d\hat{y}$, $\hat{Z}_B'\equiv d\hat{Z}_B/d\hat{y}$. There is a similar expression for the perturbed shock boundary.[15,16,34] As indicated earlier, $\tilde{\phi}_0$, $\tilde{\phi}_1$, and $\tilde{\phi}_2$ are independent of $\bar{y}$. Note that the third term on the right-hand side of Eq. (21) is introduced so that the upwash effect is transferred through the solution $\tilde{\phi}_2$ to the wing surface as part of the incidence correction to $\tilde{\phi}$, whereas the second term, $\epsilon\Theta\hat{c}'\tilde{\phi}_1$, accounts only for the nonhomogeneous correction to the PDE owing to the spanwise density variation.

The equations and boundary conditions in the reduced problems for the three similarity solutions $\tilde{\phi}_0$, $\tilde{\phi}_1$, and $\tilde{\phi}_2$ can be obtained readily from Eqs. (11), and have been described in detail in Refs. 14-16 and 34. We shall not repeat it here, except to point out that the $\bar{z}$ derivatives of $\tilde{\phi}_1$ and $\tilde{\phi}_2$ on the wing are required to be zero and unity, respectively, and that the upwash function $\tilde{C}_l^i$ in Eq. (21) is determined from $\hat{C}_l^i$ as

$$\tilde{C}_l^i=\hat{C}_l^i-\frac{\Theta}{2K_n}\frac{\tilde{\Gamma}_0}{\pi}\hat{c}'\ell n\hat{c} \qquad (22)$$

IV. Examples and Comparisons with Full-Potential Solutions

Inasmuch as the existence and uniqueness of the solutions cannot be easily investigated, demonstration of numerical solutions to the reduced problem is an essential part of the study.

Remarks on Existing 3-D Potential Computer Code

The crude description of the far field in most discretized flowfield computation methods is well known. This problem becomes more serious in the 3-D cases.[23-29] It is not all clear from the published data whether the grid distributions used therein are sufficiently refined for the purpose of adequately describing the upwash induced by the far-wake vorticity, which is crucial in the analysis of high aspect ratio wings.

There appears to be an additional problem brought about by the scarcity of the span stations available in current 3-D potential-flow programs.[25-29] In the computer code for planar wings based on Ref. 26, referred to by most users as "FLO 22," a total of 21 span stations are allowed. Applying it to an oblique wing, for example, there remains only 10 stations on each wing panel, with the wing tip represented by a trapezoid. Therefore, one cannot attach too much confidence to the numerical data obtained for the tip region.¶ It has also been known among users that the span load and sectional lift coefficient are far from being smooth—the values at successive stations appear to alternate about some mean-value curve. Figure 4 shows typical results of a sectional lift coefficient obtained from the converged solutions generated by two versions of the FLO 22 code for a 6% thick elliptic wing pivoted at 22.5 deg at $M_\infty=0.824$. The irregularity mentioned is clearly noticeable and requires some caution in making comparisons. The code is, nevertheless, known to be capable of reproducing the span loads determined by the (linear) panel methods in the subsonic range.[29]

Presumably, this irregularity has not been observed in the 3-D computations using the transonic small-disturbance (TSD) equations[24]; however, existing 3-D TSD codes are not directly applicable to problems lacking a bilateral symmetry, such as that of an oblique wing. Furthermore, the small-disturbance assumption breaks down near the leading edge; comparison with the TSD code will not reveal the important limitations of the present (small-disturbance) theory. For the above two reasons, comparison with the TSD codes has not been made. Nevertheless, we believe such a comparison could be quite useful in future studies involving shocks.

From a theoretical viewpoint, a limitation of current 3-D full-potential codes appears to be the empiricism introduced by the modeling of the inviscid wake, which we believe could have been avoided. Two assumptions on the vortex sheet were implicit in Refs. 25-28: 1) the shape of the trailing vortex sheet is specified a priori; and 2) a condition equivalent to

$$\left(\frac{\partial^2\phi}{\partial z^2}\right)_{TV}=0 \qquad (23)$$

is applied at the TV sheet.** Assuming a thin airfoil section, assumption 1 is seen to be equivalent to that in the TSD theory, in which the TV sheet is transferred to the "wing trace" on the x axis. Condition 2 is incorrect strictly speaking, since $\partial^2\phi/\partial z^2$ is generally discontinuous at the sheet. In fact, Eq. (23) would lead to

$$\left(\frac{\partial^2\phi}{\partial y^2}\right)_{TV}=0 \qquad (24)$$

far downstream, which would admit only span loadings represented by a second-degree polynomial. Apparently, a central-difference approximation was applied to Eq. (23) in Refs. 25-28, stipulating that $\partial^2\phi/\partial z^2$ was continuous at the sheet. This then gives

$$\left(\frac{\partial\phi}{\partial z}\right)_{TV}^{+}-\left(\frac{\partial\phi}{\partial z}\right)_{TV}^{-}=0 \qquad (25)$$

that is, the upwash is continuous across the wing trace, which is the correct requirement according to the TSD theory. Therefore, current codes based on Refs. 25-28 do not correspond to the exact full-potential solution.

Computations of $\tilde{\phi}_0$, $\tilde{\phi}_1$, and $\tilde{\phi}_2$

The reduced mixed-type problems for the similarity solutions $\tilde{\phi}_0$, $\tilde{\phi}_1$, and $\tilde{\phi}_2$ are solved numerically by a relaxation method, using type-sensitive difference operators corresponding to Murman's "fully conservative form."[42]

¶There is a similar question on truncation errors near the symmetry plane of a symmetric swept wing, which are amplified by the singularity of the coordinate transformation.

**This controversial condition was brought to our attention by Norman D. Malmuth.

The procedure of line relaxation used for $\tilde{\phi}_0$ may be considered standard, except for the uses of an improved far-field description and a third-order convergence acceleration scheme.[43] Inasmuch as the cases studied below are shock-free, the shock-fitting algorithm[44] and shock-perturbation analysis will not be discussed. A more complete description of the solution procedure and solution examples for $\tilde{\phi}_0$, $\tilde{\phi}_1$, and $\tilde{\phi}_2$ in the shock-free cases have been given in Ref. 16 (see also Sec. 5.2 of Ref. 34).

Examples: Comparison with Solutions Based on the Full-Potential PDE

For the purpose of comparing the lifting-line analysis (the similarity solution structure, in particular) with the corresponding full-potential solutions, we will now consider examples of high subcritical and slightly supercritical component flows over oblique as well as symmetric swept wings. The wing planforms considered are all elliptic, with the major axis coinciding with the midchord (50%); the wing sections are generated from a single profile NASA 3612-02, 40, rescaled to an arbitrary thickness τ; the latter is equated to α in the theory. These wings fulfill the geometrical description of Eqs. (8) and (19); therefore, the inner solution can be obtained by a linear combination of the basic similarity solutions $\tilde{\phi}_0$, $\tilde{\phi}_1$, and $\tilde{\phi}_2$, which will be determined after specifying the component transonic parameters K_n, the ratio of incidence to the thickness ratio, and the locations of the leading and trailing edges. Note that this airfoil has been used in various wind tunnels and preliminary design studies of oblique wings at $M_\infty = 0.60$-1.4.[11,45] Several sets of basic similarity solutions have been obtained for $K_n = 3.6$ and 3.45 for this airfoil, and have been described in some detail in Refs. 12-16. These solutions are used in the subsequent comparison with the full-potential solutions. The case with $K_n = 3.45$ is slightly supercritical.

Numerical results comparable with our solutions are generated from one version of Jameson-Caughey 3-D, full-potential computer codes, "FLO 22" (see Refs. 6, 25, and 26), which was modified slightly for oblique-wing analyses at NASA Ames Research Center and Grumman Aerospace Corporation. The different algorithms employed in FLO 22 are not fully conservative, but this may not be essential for shock-free solutions presented below. We point out that the FLO 22 data from NASA Ames and Grumman are not identical, owing to the differences in the mesh size, spacing of the span stations, convergence criteria, and the detail of the leading-edge description. The availability of data from two sources is helpful in delineating the nature of discrepancy between our theory and the more exact 3-D programs.

A number of FLO 22 runs have been made for the oblique wings with freestream Mach number, swept angle, wing thickness, etc., chosen to give either $K_n = 3.6$ or $K_n = 3.45$, employing the same basic airfoil section. An elliptic planform is used in each case; wing twist and wing bend are assumed to be zero. Among the first comparison studies made is a case with relatively thin wing section (6% thickness ratio) and a rather high aspect ratio (major-to-minor axes ratio of 20). The surface pressure coefficients in this case have been presented in Ref. 15 (see also Fig. 9 of Ref. 34). The freestream Mach number and the sweep angle used in the FLO 22 calculation therein are $M_\infty = 0.8242$ and $\Lambda = 22.5$ deg, giving a component Mach number $M_n = 0.7615$. Thus, one has $K_n = 3.60$, $\Theta = 1.003$, and $\epsilon = 0.1277$ in this case; the component flow is slightly below being critical. There, the FLO 22 data from NASA Ames and Grumman appear to be rather close except next to the leading edge. The C_p values computed from the similarity solutions agree reasonably well with the FLO 22 data except near the leading edge.[15,16]

The degree of agreement between the FLO 22 data and the theory does not appear to deteriorate much with increasing wing thickness or reducing wing aspect ratio. The consolidated plot in Fig. 5 shows the surface pressure coefficient at seven span stations on a 12% thick, 14:1 elliptic wing, pivoted at $\Lambda = 30$ deg for $M_\infty = 0.7677$. The component Mach number is $M_n = 0.6648$ in this case, giving $K_n = 3.45$. The

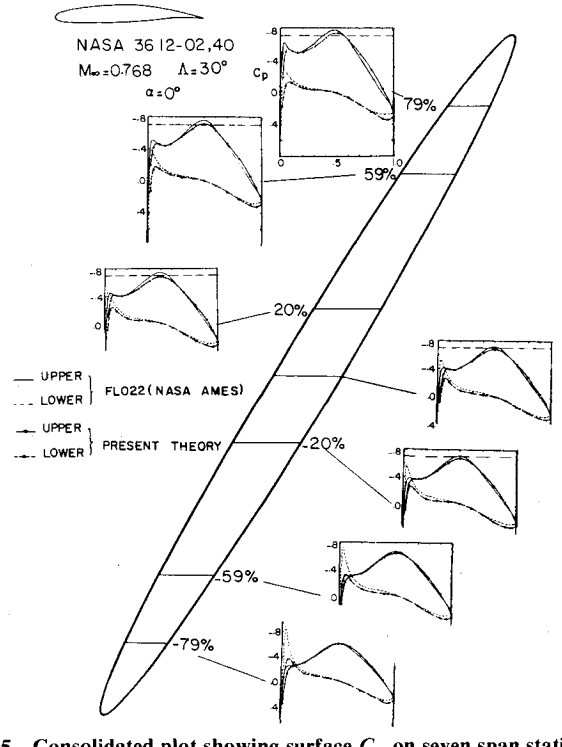

Fig. 5 Consolidated plot showing surface C_p on seven span stations of an oblique wing pivoted at 30 deg at flight Mach number 0.767. The planform is a 14:1 ellipse; the wing section is NASA 3612-02, 40, zero incidence, zero twist, and zero wing bend.

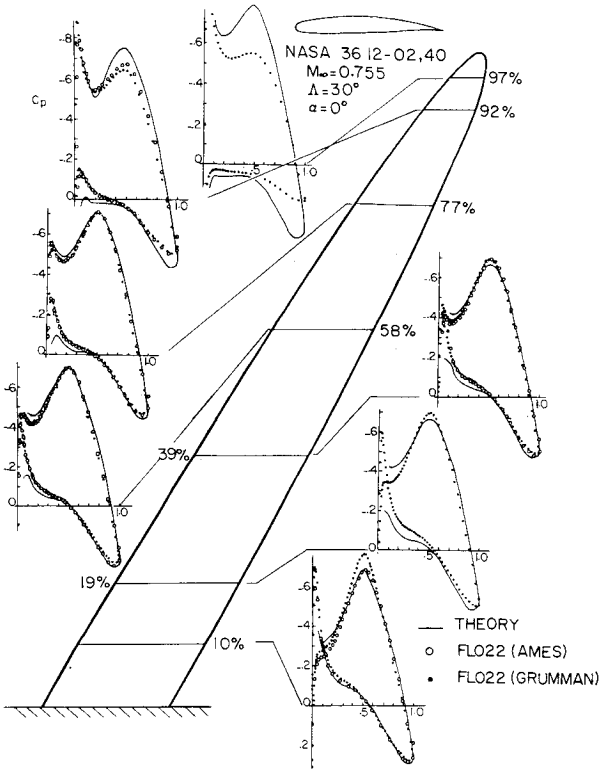

Fig. 6 Consolidated plot showing surface C_p on seven span stations of a symmetric swept-back wing with 30 deg sweep angle at flight Mach number of 0.755. The basic planform is a 14:1 ellipse; the wing section is NASA 3612-02, 40, zero incidence, zero twist, and no wing bend.

three sets of surface data, $\tilde{\phi}_{0\bar{x}}$, $\tilde{\phi}_{1\bar{x}}$, and $\tilde{\phi}_{2\bar{x}}$, are used to construct the C_p distributions. The C_p value for the component flow is -0.689 and both FLO 22 and lifting-line solutions give the appearance of supercritical shock-free regions on the upper surface of the downstream wing panel.

The agreement between the FLO 22 data and those based on the asymptotic analysis in Refs. 15 and 16 and in Fig. 5 should be considered as being better than expected, inasmuch as the relative error in the asymptotic theory belongs to an order determined by $\tau^{2/3}$ or ϵ^2, whichever is larger. The magnitude of $\tau^{2/3}$ for the examples shown in Fig. 5 is 0.243. It may be recalled in this connection that there is a noticeable difference between the two sets of FLO 22 data for the local lift coefficient shown earlier in Fig. 4.

It is not altogether clear that the encouraging agreement found for the oblique wings may still hold to some degree with the presence of an apex in a symmetric swept wing, where the theory must fail. Figure 6 presents a consolidated plot for surface pressure coefficient at seven span stations on a symmetric swept wing with the same basic (elliptic) planform, sweep angle, and section profile as those in the preceding figure. The freestream Mach number is, however, slightly lower with $M_\infty = 0.7549$; thus, $M_n = 0.6538$, $K_n = 3.60$, $\epsilon = 0.1448$, and $\Theta = 1.062$. The solution remains subcritical component-wise for most stations (the dashed line in Fig. 6 indicates $C_p = -0.727$, where the local component Mach number reaches unity). The stations $\bar{y} = 0.92$ and 0.97 are included to illustrate the solution behavior near the tip, where the trends of departure of the asymptotic (lifting line) from the FLO 22 analyses, as well as between the two sets of FLO 22 data themselves, are evident. Away from the tip, agreement is as reasonable as in the two preceding comparisons for the oblique wings. However, the set of FLO 22 data in filled circles gives a consistently higher peak for $-C_p$ than the one in open circles. The discrepancy may be associated with the uncertainty related to the fluctuating spanwise distributions of sectional lift shown in Fig. 4. The present theory tends to give a consistently lower $-C_p$ than the FLO data on the lower surface around the quarter chord. This tendency is also apparent from Fig. 5. This small, but noticeable, discrepancy may be associated with the accuracy and degree of convergence in the $\tilde{\phi}_0$ solution.

The most important piece of information from Fig. 6 is the comparison made for the station closest to the apex. At 10% semispan from the symmetry plane ($\bar{y} = 0.097$), the agreement of the asymptotic results with the FLO 22 data (in open circles) remains as good as other stations. The discrepancy in the vicinity of the apex is seen to be less than that in the tip region; the latter is believed to arise partly from the treatment of the wing-tip geometry by the FLO 22 code mentioned earlier. In passing, we remark that near the symmetry plane where the leading-edge sweep angle has a discontinuity, even the full-potential code may not be strictly reliable owing to the scarcity of span stations (cf. footnote, third paragraph Sec. IV).

V. Concluding Remarks

The foregoing presentation has shown that Prandtl's lifting-line idea, originally applied to an unyawed, straight wing of high aspect ratio, can be extended to the study of 3-D mixed flows over transonic swept wings. Examples of oblique and symmetric swept wings involving the high subcritical and slightly supercritical component flows are shown; comparisons with full-potential solutions from an existing computer code are made. Except near the wing tip and root and the leading edge, where breakdowns in either the theory or the code are expected, the agreement with the full-potential results is encouraging.

An important feature of the analysis is the upwash correction proportional to $\epsilon\ell_n\epsilon\Theta(d\bar{\Gamma}/d\bar{y})$, resulting from the spanwise ($y'-$) component of the locally shedded wake vorticity. The dependence of the upwash correction on the sweep and the span loading have been shown. A significant gain in the theoretical development through this approach is the availability of a similitude in the 3-D flow structure applicable to wings with sections generated from a single profile. With the similarity solutions, the reduced 2-D problems are solved only once for all span stations. From these and the upwash analysis, the dependence of the flowfield on wing sweep, aspect ratio, local chord variation, as well as the twist and the bend, can be explicitly studied, thus furnishing a rational tool for transonic aerodynamic design.

The examples studied in this paper do not include examples with embedded shocks. Solutions making use of the 3-D corrections for the shock jump and the shock geometry have been obtained, and their comparison with full-potential results will be discussed in a sequel paper. Omitted from the foregoing discussion is the feasibility of solutions via a special unsteady analogy. Unpublished results computed from this analogy with an ADI algorithm by T. Evans of the University of East Anglia compare rather closely with similarity solutions, and promise an effective procedure for treating more complicated shock patterns.[16,35]

Whereas local treatment of the leading-edge breakdown in the small-disturbance theory is possible,[46] an alternative solution to this difficulty is to develop a lifting-line theory on the basis of the potential theory without the small-disturbance assumption. Work along this line has been carried out in Ref. 36, where, interestingly, solutions via similarity flow structure may again be found. Treatment of nonuniformities at the root and along the tip are the remaining problems for the lifting-line theory in linear and nonlinear regimes; their analyses for the transonic regime would involve solving a fuller reduced 3-D problem.

Acknowledgment

The material in this paper is taken partly from studies supported by the Office of Naval Research, Fluid Dynamics Program (Contract N00014-75-C-0520). Most computation work related to the FLO 22 code was carried out at the NASA Ames Research Center under the joint study programs with the University of Southern California (through Agreements NCR-530-501 and NCA 200R-730-601) and at Grumman Aerospace Corporation. We are pleased to acknowledge the valuable advice on the oblique wing study by R. T. Jones and the use of the FLO 22 code by T. Jameson, R. M. Hicks, A. Levin, and R. Lasslo.

References

[1] Busemann, A., "Aerodynamischer Auftrieb bei Überschallgeschwindigkeit," *Lüftfuhrtforschung*, Vol. 12, No. 6, 1975, pp. 210-220.

[2] Jones, R. T., "Wing Planform for High Speed Flight," NACA Rept. 863, 1945.

[3] Jones, R. T. and Cohen, D., "Aerodynamics of Wings at High Speed," in *Aerodynamic Components of Aircraft at High Speed*, edited by D. F. Donovan and H. R. Lawrence, Princeton University Press, Princeton, New Jersey, 1957.

[4] Küchemann, D., "Aerodynamic Design," *The Aeronautical Journal*, Vol. 73, 1968, p. 101.

[5] Jones, R. T., "Reduction of Wave Drag by Antisymmetric Arrangement of Wings and Bodies," *AIAA Journal*, Vol. 10, Feb. 1972, pp. 171-176.

[6] Bauer, F., Garabedian, P. R., Korn, D. G., and Jameson, A., *Supercritical Wing Section,* 11, Lecture Notes in Economics and Mathematical Systems, No. 108, Springer-Verlag, Berlin, 1974.

[7] Nieuwland, G. Y. and Spee, B. M., "Transonic Airfoils: Recent Developments in Theory, Experiment and Design," *Annual Review of Fluid Mechanics*, Vol. 5, 1973, pp. 119-150.

[8] Boerstoel, J. W., "A Transonic Hodograph Theory for Airfoil Design," National Aerospace Laboratory Rept. NLRMP 74024 U, Amsterdam, Netherlands, Sept. 1974.

[9] Kacprzynski, J. J., Ohman, L. H., Garabedian, P. R., and Korn, D. G., "Analysis of the Flow Past a Shockless Lifting Airfoil in Design and Off-Design Conditions," National Research Council of Canada, Aeronautical Rept. LR-554, Ottawa, 1971.

[10] Whitcomb, R. T., "Review of NASA Supercritical Airfoils," *Proceedings of the 9th International Congress on Aeronautical Sciences*, Haifa, Israel, 1974.

[11] Jones, R. T., "The Oblique Wing: Aircraft Design for Transonic and Low Supersonic Speeds," *Acta Aeronautica*, Vol. 4, Jan. 1977, pp. 99-110.

[12] Cheng, H. K., "Lifting-Line Theory for Oblique Wings," *AIAA Journal*, Vol. 16, Nov. 1979, pp. 1211-1213.

[13] Cheng, H. K., "Theory of Oblique Wings of High Aspect Ratio," University of Southern California, School of Engineering, Dept. of Aerospace Engineering, Rept. USCAE 135, Aug. 1978.

[14] Cheng, H. K. and Meng, S. Y., "Lifting-Line Theory for Oblique Wings in Transonic Flows," *AIAA Journal*, Vol. 17, Jan. 1979, pp. 121-124.

[15] Cheng, H. K. and Meng, S. Y., "The Oblique Wing as a Lifting-Line Problem in Transonic Flow," *Journal of Fluid Mechanics*, Vol. 97, Pt. 3, 1980, pp. 531-556.

[16] Cheng, H. K. and Meng, S. Y., "The Oblique Wing as a Lifting-Line Problem in Transonic Flow," University of Southern California, School of Engineering, Dept. of Aerospace Engineering, Rept. USCAE 136, May 1979.

[17] Cook, L. P. and Cole, J. D., "Lifting-Line Theory for Transonic Flow," *SIAM Journal of Applied Mathematics*, Vol. 35, Sept. 1978, pp. 209-224.

[18] Cook, L. P., "A Uniqueness Proof of a Transonic Flow Problem," *Indiana University Mathematics Journal*, Vol. 27, No. 1, 1978.

[19] Small, R. D., "Transonic Lifting-Line Theory: Numerical Procedure for Shock-Free Flows," *AIAA Journal*, Vol. 16, June 1978, pp. 632-634.

[20] Cook, L. P., "Lifting-Line Theory for a Swept Wing at Transonic Speeds," *Quarterly Applied Mathematics*, July 1979, pp. 178-202.

[21] Prandtl, L., "Traflügeltheorie," *Nachrichten d.k. Gesellschaft d. Wiss* 24, Göttingen, Math-Phys Klass, 1918, pp. 451-477.

[22] Van Dyke, M. D., "Lifting-Line Theory as a Singular Perturbation Problem," *Archiwum Mechaniki Stosowanej*, Vol. 16, No. 3, 1964, pp. 601-614; *Journal of Applied Mathematics and Mechanics*, Vol. 28, 1964, pp. 90-101.

[23] Ballhaus, W. F., "Some Recent Progress in Transonic Flow Computations," presented at the Lecture Series on Computational Fluid Dynamics, von Kármán Institute, Rhode-St.-Genese, Belgium, March 1976.

[24] Bailey, F. R. and Ballhaus, W. F., "Comparison of Computed and Experimental Pressures for Transonic Flows about Isolated Wings and Wing-Fuselage Configurations," NASA SP-347, Pt. 11, 1975, pp. 1213-1231.

[25] Jameson, A., "Iterative Solution of Transonic Flows over Airfoils and Wings, Including Flows at Mach 1," *Communications on Pure and Applied Mathematics*, Vol. 27, 1974, pp. 283-309.

[26] Jameson, A. and Caughey, D. A., "Numerical Calculations of the Transonic Flow Past a Swept Wing," Courant Inst. Math. Sciences, ERDA Math. Computing Lab. Rept. C00-3077-140, June 1977.

[27] Jameson, A. and Caughey, D. A., "A Finite Volume Method for Transonic Potential Flow Calculations," *Proceedings of AIAA 3rd Computational Fluid Dynamics Conference,* Albuquerque, N. Mex., June 1977, pp. 35-54.

[28] Caughey, D. A. and Jameson, A., "Numerical Calculations of Potential Flow About Wing-Body Combinations," *AIAA Journal*, Vol. 7, Feb. 1979, pp. 175-181.

[29] Henne, P. A. and Hicks, R. M., "Transonic Wing Analysis Using Advanced Computations Methods," Douglas Aircraft Co., McDonnell Douglas Corp., Douglas Paper 6647, 1979.

[30] Weissinger, J., "Ueber die Auftriebsverteilung von Pfeilflügeln," FB 1553, Berlin-Adlershof, 1942; NACA TM 1120, 1947.

[31] Krienes, K., "The Elliptic Wing Based on the Potential Theory," *ZAMM*, Vol. 20, No. 2, 1939, pp. 65-88; NACA Tech. Memo 97, 1970.

[32] Dorodnitsyn, A. A., "Generalization of the Lifting-Line Theory for Cases of a Wing with a Curved Axis and a Slipping Wing," *Prikladnaya Mathematikai Mechanika*, Vol. 8, 1944, pp. 33-64.

[33] Thurber, J., "An Asymptotic Method for Determining the Lift-Distribution on a Swept-Back Wing of Finite Span," *Communications on Pure and Applied Mathematics*, Vol. 18, 1965, pp. 733-750.

[34] Cheng, H. K., Meng, S. Y., Chow, R., and Smith, R. C., "Transonic Swept Wing Analysis Using Asymptotic and Other Numerical Methods," AIAA Paper 80-0342, Jan. 1980; also distributed with revised errata sheet as University of Southern California, School of Engineering, Dept. of Aerospace Engineering, Rept. USCAE 138, May 1980.

[35] Cheng, H. K., "The Transonic Flow Theories of High and Low Aspect Ratio Wings," *Physical and Numerical Aspects of Aerodynamic Flows*, Calif. State Univ., Long Beach, Calif., Jan. 1981.

[36] Cheng, H. K., Chow, R., and Melnik, R. E., "Lifting-Line Theory of Swept Wings Based on the Full Potential Theory," submitted to ZAMP.

[37] von Kármán, T., "The Similarity Law of Transonic Flow," *Journal of Mathematical Physics*, Vol. 26, 1947, pp. 182-190.

[38] Murman, E. M. and Cole, J. D., "Calculation of Plane Steady Transonic Flows," *AIAA Journal*, Vol. 9, Jan. 1971, pp. 114-121.

[39] Cole, J. D., "Modern Development in Transonic Flows," *SIAM Journal of Applied Mathematics*, Vol. 29, No. 4, Dec. 1975, pp. 763-787.

[40] Murman, E. M. and Krupp, J. A., "Solutions of the Transonic Potential Equation Using a Mixed Finite-Difference System," *Proceedings of 2nd International Conference on Numerical Methods in Fluid Dynamics*, Lecture Notes in Physics, Springer-Verlag, Berlin-Heidelberg, New York, 1971, pp. 199-206.

[41] Jones, R. T., "The Spanwise Distribution of Lift for Minimum Induced Drag of Wings Having a Given Bending Moment," NACA TN 2249, 1950.

[42] Murman, E. M., "Analysis of Embedded Shock Waves Calculated by Relaxation Methods," *AIAA Journal*, Vol. 12, Dec. 1974, pp. 626-633.

[43] Meng, S. Y. and Cheng, H. K., "Convergence Acceleration of Relaxation Solutions by the Power Method: Higher-Order Algorithms," *Proceedings of Applied Computer Methods in Engineering*, edited by L. C. Wellford, University of California, Los Angeles, Calif., 1977, pp. 395-404.

[44] Hafez, M. M. and Cheng, H. K., "Shock-Fitting Applied to Relaxation Solutions of Transonic Small-Disturbance Equations," *AIAA Journal*, Vol. 15, June 1977, pp. 786-793.

[45] Black, R. L., Beamish, J. K., and Alexander, W. K., "Wind Tunnel Investigations of an Oblique-Wing Transport Model at Mach Number Between 0.6 and 1.4," NASA CR-137 697, HST-TR-344-0, July 1975.

[46] Keyfitz, B. L., Melnik, R. E., and Grossman, B., "An Analysis of the Leading-Edge Singularity in Transonic Small Disturbance Theory," *Quarterly Journal of Mechanics and Applied Mathematics*, Vol. 31, Pt. 2, May 1978, pp. 137-155.